Non-linearity of rockglacier flow law determined from geomorphological observations:

A case study from the Murtèl rockglacier (Engadin, SE Switzerland)

Marcel Frehner[1], Dominik Amschwand[1] and Isabelle Gärtner-Roer[2]

[1]Geological Institute, ETH Zurich, Switzerland (marcel.frehner@erdw.ethz.ch)
[2]Department of Geography, University of Zurich, Switzerland

1 Introduction

The creep behavior (rheology) of rockglaciers may deviate from the well-known flow-law for pure ice. Here we constrain the non-linear flow law governing rockglacier creep based on borehole deformation data and geomorphological criteria. The Murtèl rockglacier (upper Engadin valley, SE Switzerland) serves as a case study, for which high-resolution DEMs, time-lapse borehole deformation data, and geophysical soundings exist that reveal the exterior and interior architecture and dynamics of the landform.

Borehole inclination data of the Murtèl rockglacier (Arenson et al., 2002) reveal a curved deformation profile. In map view, the prominent furrow-and-ridge morphology also exhibits a curved geometry. Hence, the surface morphology and the borehole deformation data together describe a curved 3D flow geometry. Frehner et al. (2015) reproduced the curved vertical flow profile and the furrow-and-ridge morphology (yet neglecting its curved geometry in map view) using a 2D linear viscous (Newtonian) flow model.

Linear viscous models result in perfectly parabolic flow geometries; non-linear creep leads to localized deformation at the bottom and sides of the rockglacier while the deformation at the top and in the interior are less intense. In other words, non-linear creep results in non-parabolic flow geometries. By comparing the curved 3D flow geometry with theoretical 3D flow geometries, we determine the most adequate flow-law that fits the natural deformation geometry best.

2 The Murtèl rockglacier

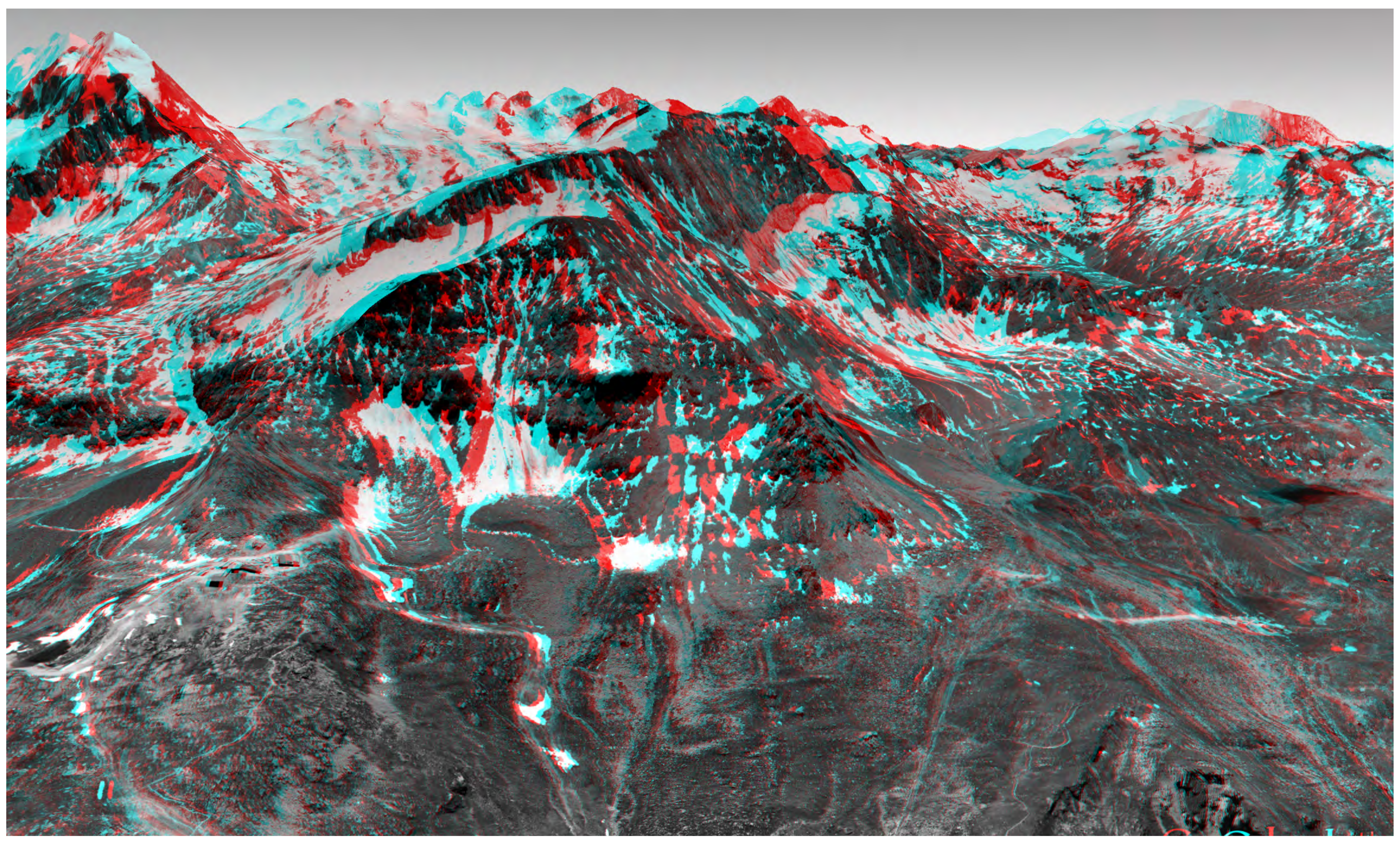

↑ *Fig. 1: Regional overview (Google Earth) of Piz Corvatsch and the Murtèl cirque. Grab a pair of red-blue 3D glasses. Important: Relax your eyes; e.g. focus on the furthest peaks right of the center of the image.*

3 Motivation: Our previous work

In Frehner et al. (2015), we applied the buckle folding theory for linear viscous (Newtonian) materials to explain the furrow-and-ridge morphology on the Murtèl rockglacier. Based on the spacing of the furrows and ridges (L≈20 m) we determined the effective (Newtonian) viscosity ratio between the upper layer (h=3 m) and the main rockglacier body as R=21.

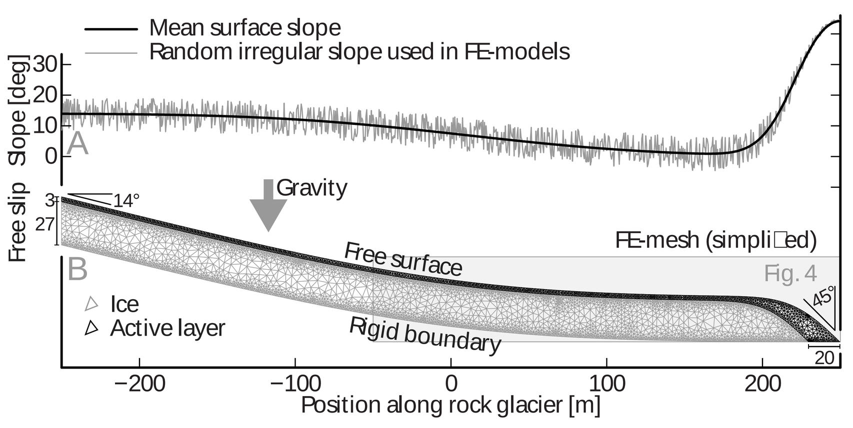

Buckle folding theory in a nutshell: Buckle folding is the mechanical response of layered viscous materials to layer-parallel compression. The wavelength (L) depends on the viscosity ratio (R) between the stiff (folded) and soft layer and on the thickness of the stiff layer (h).

← *Fig. 2: 2D linear viscous finite- element model based on the Murtèl rockglacier (h=3 m, R=21).*
↙ *Fig. 3: The simulation reproduces Murtèl's furrow-and-ridge morphology (L≈20 m) and the upper part of the curved borehole deformation profile.*

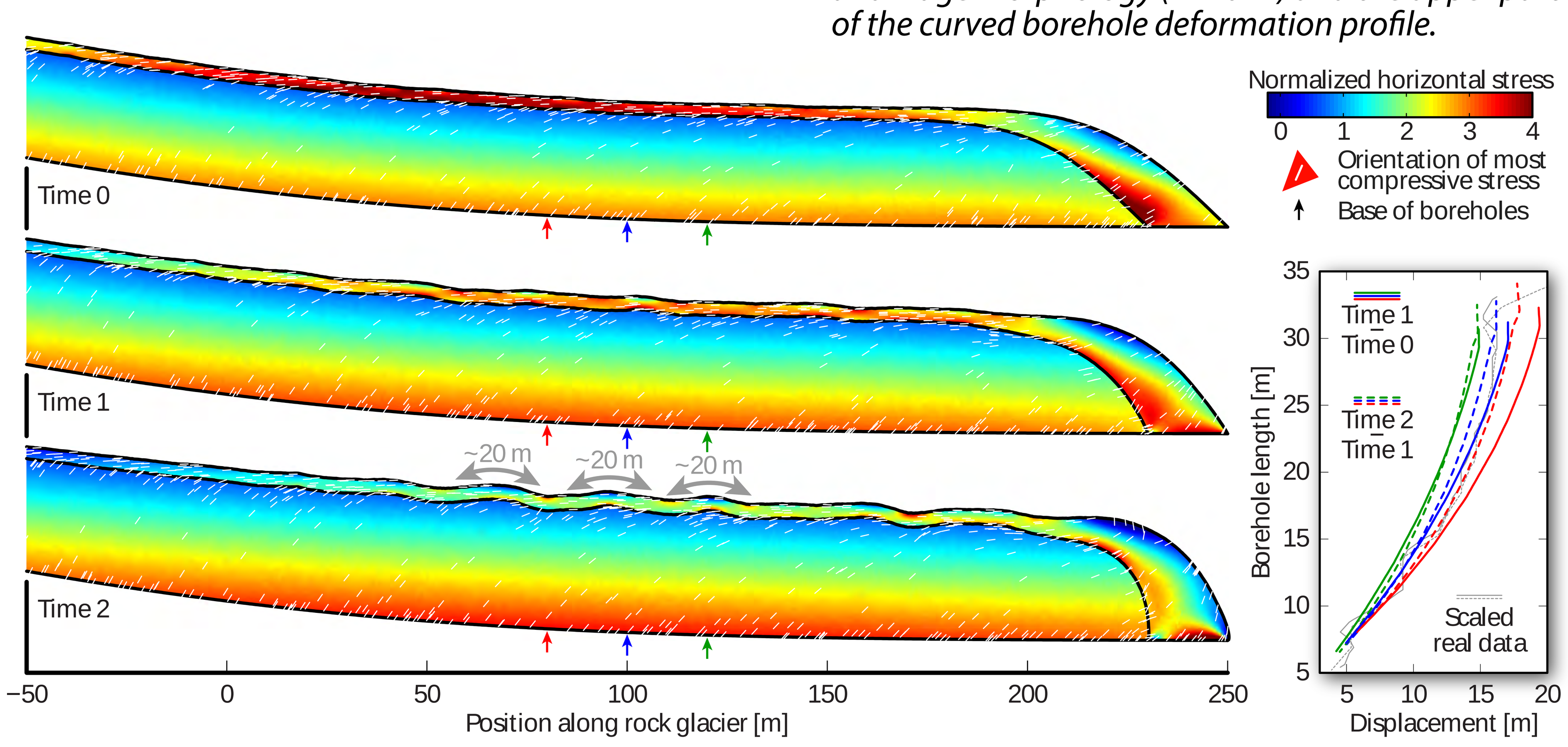

4 Used data

→ *Fig. 4: Differential elevation calculated from a 1 m resolution DEM (Frehner et al., 2015). We also use a drone-based 8 cm resolution DEM. The curved furrow-and-ridge morphology is clearly visible.*
→→ *Fig. 5: Borehole deformation data (Arenson et al., 2002) highlighting the curved flow geometry above the basal shear zone at ~30 m depth.*

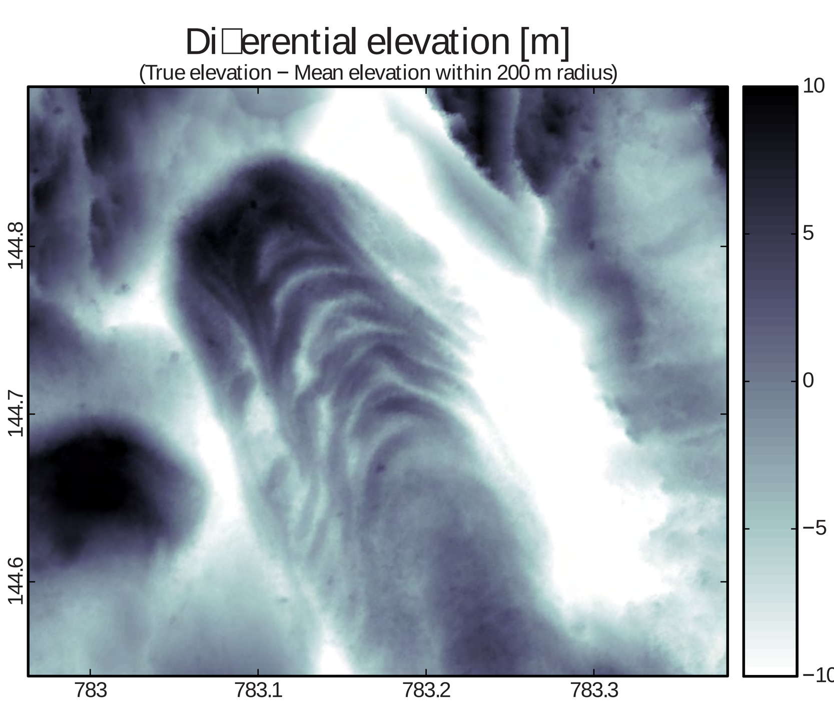

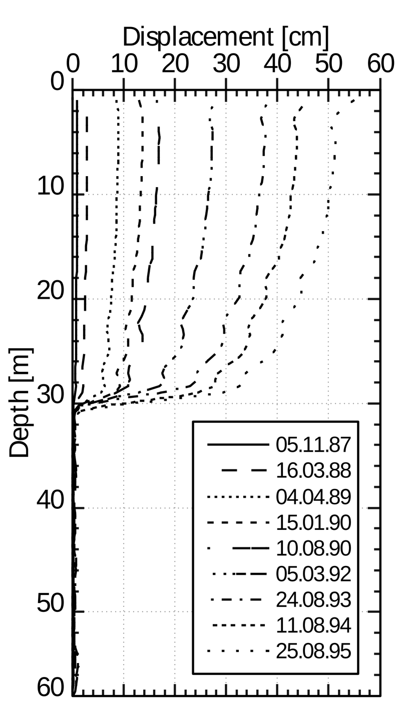

5 Basic research idea and workflow

Flow of non-linear viscous materials leads to curved, but not perfectly parabolic flow structures. Ideally, the **power-law exponent of the curved flow structures** (m) is **one unit larger than** the **power-law stress exponent of the non-linear rheological flow law** (n). Hence, the following relationship applies:

Rheological flow law (Glen's (1952) flow law): $\tau^n = A\dot{\varepsilon}$
↳ Geometry of furrow-and-ridge morphology: ↳ $u_x(y) = Bx^{n+1} = Bx^m$
↳ Horizontal borehole deformation with depth: ↳ $u_x(z) = Cz^{n+1} = Cz^m$

τ: shear stress, $\dot{\varepsilon}$: shear strain rate, u_x: displacement in flow direction, x: flow direction, y: direction perpendicular to flow, z: depth, A, B, C: material or geometrical constants.

Therefore, **geometrical analysis** of **curved furrow-and-ridge morphology** in map view (Fig. 4) and the **curved borehole deformation data** in vertical view (Fig. 5) should allow **determinining the power-law exponent** (n) governing the viscous flow. Various assumptions and boundary conditions may be applied:

- In map view: consider the entire furrow-and-ridge structure or reject few meters on each side
  In the borehole: include or reject the top 5 m and/or bottom few meters (shear zone)
- Fixed value(s) or or fixed gradient(s) at the end(s) of the structure (e.g., at the top of the borehole)

6 First results for borehole data

So far, we analyzed two borehole curves (Fig. 6 & 7, Table 1). Considering the **entire borehole**, the **power-law fit performs significantly better** (R^2>0.92) **than the quadratic fit** (R^2<0.75) and we find **power-law exponents of 5.14>m>7.30**. Considering **only the middle section** of the borehole, all different fitting curves perform equally well (R^2>0.96) and we find **power-low exponent close to m=2**.

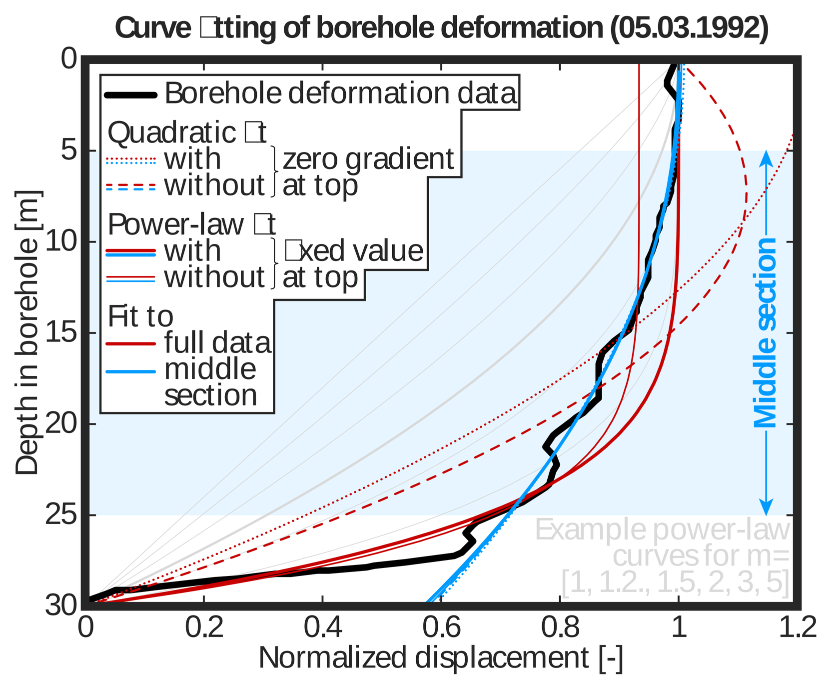

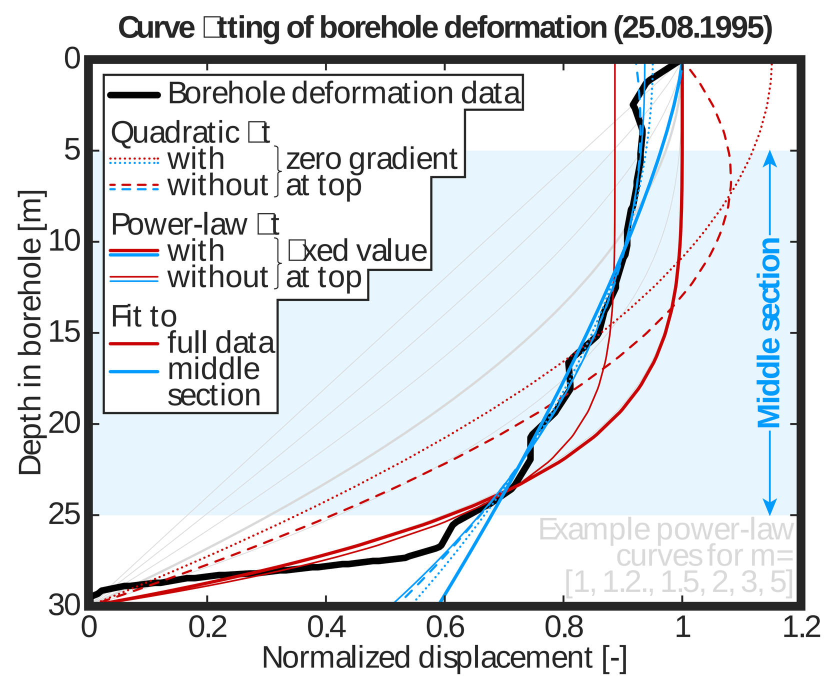

		Quadratic fit						Power-law fit			
Fit to entire borehole		✓	✓	✓				✓	✓		
Fit only to middle section					✓	✓	✓			✓	✓
Fixed bottom [d(30 m) = 0]		✓	✓	✓				✓	✓		
Fixed top [d(0 m) = 1]		✓		✓			✓	✓		✓	
Zero gradient at top [dd(0 m)/dz = 0]			✓	✓		✓	✓	✓	✓	✓	✓
Symbol in Fig. 6 & 7		red dashed	red dotted	grey solid	blue dashed	blue dotted		red thick	red thin	blue thick	blue thin
05.03. 1992	m=	2 (forced)						6.06	7.30	2.19	2.10
	R^2=	0.71	0.58	0.38	0.98	0.98	0.98	0.94	0.96	0.98	0.98
25.08. 1995	m=	2 (forced)						5.14	6.75	1.36	2.37
	R^2=	0.75	0.67	0.60	0.99	0.98	0.87	0.92	0.96	0.96	0.99

↖ *Fig. 6* & ↑ *Fig. 7: Borehole deformation curves (Arenson et al., 2002) and fitting functions using different boundary conditions.*

← *Table 1: Curve fitting details. Best fits are obtained using power-law functions and fitting only the middle section of the borehole.*

7 First results for furrow-and-ridge geometry

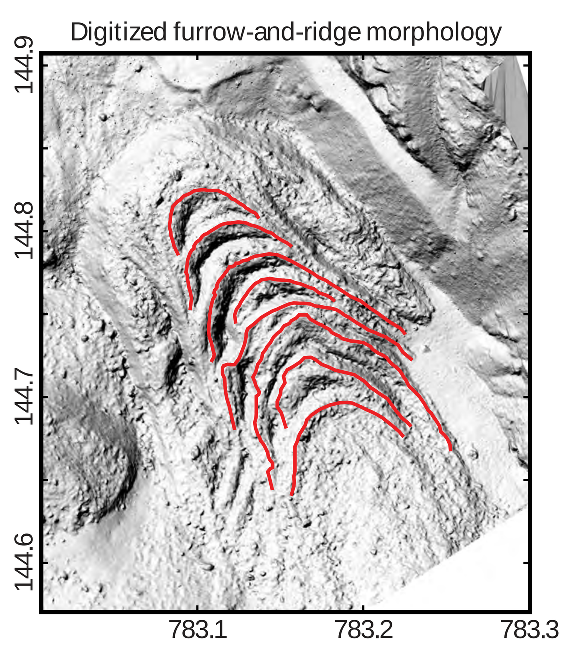

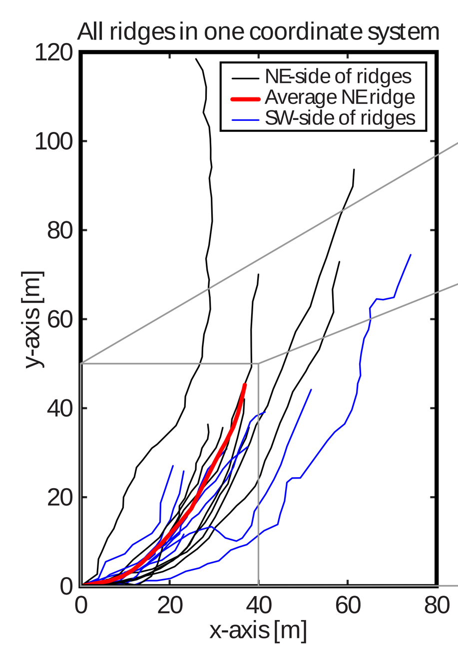

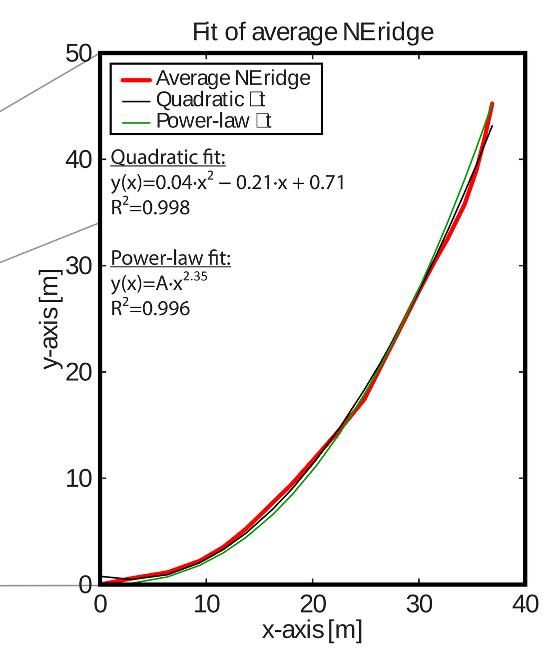

↑ *Fig. 8: Digitized curved ridges superimposed on the 8 cm DEM (hillshade). In this hillshade representation of the DEM the furrow-and-ridge morphology is particularly well visible, enabling digitization.*
↗ *Fig. 9: Digitized ridges rotated and centered into a common x-y-coordinte system. Black: ridges on the NE side of the rockglacier; Blue: ridges on the SW side; Red: calculated average ridge geometry on the NE side.*
↗↗ *Fig. 10: Average NE ridge (red) with quadratic (black) and power-law fit (green). Both fits work equally well.*

8 Discussion, Conclusions & Outlook

The **borehole deformation data** suggests that creep of the Murtèl rockglacier as a whole is governed by a **non-linear** viscous flow law with a **stress exponent (n) between 4 and 6** (i.e., m–1) (Fig. 6 & 7; Table 1). However, the rockglacier may be **divided into** a lower part with strong strain localization (**shear zone**) and the **main rockglacier body** with an almost **linear (n≈1) rheological flow law**.

The curvature of the **furrow-and-ridge morphology** suggests an almost linear (**n≈1**) **rheological flow law** (Fig. 10).

This may indicate that the development of the **furrow-and-ridge morphology is independent of the basal shear zone** and is only governed by the flow of the main rockglacier body. Such assumption has been made by Frehner et al. (2014).

Outlook

Our work continues and will be finalized during the BSc Thesis of D. Amschwand. Next, we will feed the best-fitting rheological flow law into a 3D finite-element model (Fig. 11 as example) to study the internal dynamics (stresses & strain rates) of rockglaicer flow.

↙ *Fig. 11: Different views of 3D feasibility simulation. A DEM (Fig. 4) defines the model topography. The base is equal to the 2D model (Fig. 2).*

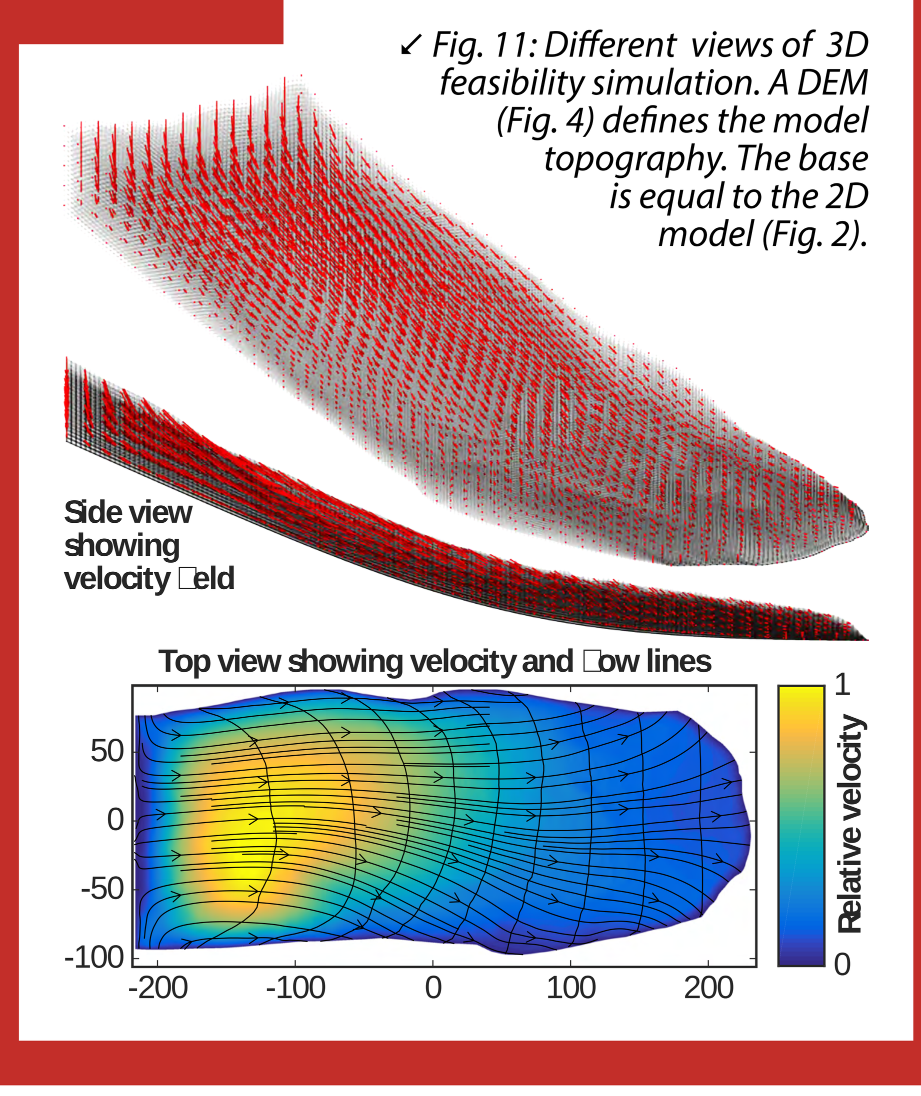

References: Arenson L. et al., 2002: Borehole deformation measurements and internal structure of some rock glaciers [...] . PPP 13, 117–135.
Frehner M. et al., 2015: Furrow-and-ridge morphology on rockglaciers explained by gravity-driven buckle folding: [...] . PPP 26, 57–66.
Glen J.W., 1952: Experiments on the deformation of ice. Journal of Glaciology 2, 111–114.

Acknowledgement: Martin Hoelzle (U. of Fribourg) for digging out the almost lost borehole deformation data.